



Published in final edited form as:

Nat Med. 2012 November ; 18(11): 1711–1715. doi:10.1038/nm.2971.

CT-based Biomarker Provides Unique Signature for Diagnosis of COPD Phenotypes and Disease Progression

Craig J. Galbán¹, Meilan K. Han², Jennifer L. Boes¹, Komal A. Chughtai¹, Charles R. Meyer¹, Timothy D. Johnson³, Stefanie Galbán⁴, Alnawaz Rehemtulla⁴, Ella A. Kazerooni¹, Fernando J. Martinez², and Brian D. Ross¹

¹Department of Radiology, University of Michigan, Center for Molecular Imaging, Ann Arbor, Michigan 48109, USA

²Department of Internal Medicine, University of Michigan, Center for Molecular Imaging, Ann Arbor, Michigan 48109, USA

³Department of Biostatistics, University of Michigan, Center for Molecular Imaging, Ann Arbor, Michigan 48109, USA

⁴Department of Radiation Oncology, University of Michigan, Center for Molecular Imaging, Ann Arbor, Michigan 48109, USA

Abstract

Chronic obstructive pulmonary disease (COPD) is increasingly being recognized as a highly heterogeneous disorder, composed of varying pathobiology. Accurate detection of COPD subtypes by image biomarkers are urgently needed to enable individualized treatment thus improving patient outcome. We adapted the Parametric Response Map (PRM), a voxel-wise image analysis technique, for assessing COPD phenotype. We analyzed whole lung CT scans of 194 COPD individuals acquired at inspiration and expiration from the COPDGene Study. PRM identified the extent of functional small airways disease (fSAD) and emphysema as well as provided CT-based evidence that supports the concept that fSAD precedes emphysema with increasing COPD severity. PRM is a versatile imaging biomarker capable of diagnosing disease extent and phenotype, while providing detailed spatial information of disease distribution and location. PRMs ability to differentiate between specific COPD phenotypes will allow for more accurate diagnosis of individual patients complementing standard clinical techniques.

Users may view, print, copy, download and text and data- mine the content in such documents, for the purposes of academic research, subject always to the full Conditions of use: http://www.nature.com/authors/editorial_policies/license.html#terms

Corresponding Author: Brian D. Ross, Ph.D., Professor of Radiology, Center for Molecular Imaging, Biomedical Sciences Research Building, Room 2071, 109 Zina Pitcher Place, University of Michigan, Ann Arbor, MI 48109-2200, Phone: (734)-763-2099, Fax: (734)-763-5447, bdross@umich.edu.

Author contributions

C.J.G. conducted data and statistical analyses and wrote the manuscript, M.K.H. acquired images, PFT data and clinical information from COPDGene, C.R.M. and J.L.B. optimized and performed image registrations, and K.S.C. aided in image registration and performed PRM on image data, T.D.J. assisted with the statistical analysis, S.G. and A.R. contributed to the design of the study and E.A.K, F.J.M. and B.D.R. supervised the project including data analysis and manuscript preparation.

Competing interest statement

C.J.G, A.R. and B.D.R. have a financial interest in the underlying technology which has been licensed from the University of Michigan to Imbio, LLC which A.R. and B.D.R. have a financial interest.

Introduction

Chronic obstructive pulmonary disease (COPD) is a highly and increasingly prevalent disorder characterized by incompletely reversible airflow limitation.^{1,2} Presently it is the fourth leading cause of death in the US, with over 11 million people suffering from the disease. The immense scope of this disease has led to major NIH-funded initiatives such as COPDGene.³ COPD is a heterogeneous disorder that arises from pathological processes including emphysematous lung tissue destruction, gross airway disease and functional small airway disease (fSAD) in varying combinations and severity within an individual. It is widely accepted that fSAD and emphysema are two main components of COPD and that a spectrum of COPD phenotypes with varying contributions of these components exists in individual patients thus the ability to diagnose the underlying phenotypes could provide for improved prognostication and treatment of individuals afflicted by this disease.^{2,4}

Computed tomography (CT) is a minimally invasive imaging technique capable of providing both high contrast and high resolution detail of the lungs and airways. CT has proven instrumental in identifying structural abnormalities associated with COPD. While most of the clinically useful information today from lung CT comes from qualitative visual inspection, extensive research has been devoted to the application of quantitative techniques to high resolution CT data sets using a wide variety of quantitative CT-based metrics to define COPD structural abnormality and disease severity. Well accepted for identifying and quantifying the emphysema component of COPD, the percentage of emphysema is determined using an attenuation-based method in which the sum of all image voxels, the smallest measurable unit of volume in an image data set, less than -950 Hounsfield Units (HU) is normalized by the total lung volume on the inspiratory CT scan.^{5,6} This metric is easily calculated from data acquired using standard imaging protocols. However, this metric only identifies one component of the heterogeneous COPD process. The second component, functional small airway disease, remains a quantitative CT challenge due to the complexity of the histopathological features of COPD affected lung tissue. Other attenuation-based techniques, such as the sum of all image voxels less than -856 HU normalized by the total lung volume on the expiratory CT scan, have been proposed as a measure of gas trapping (GT) but are unable to distinguish the contributions of small airways disease and emphysema from the GT measurement.³ This challenge has prompted research that strives towards a more accurate and complete quantitative tool for the evaluation of COPD.⁷⁻¹⁵

The motivation for the present study was to develop a robust CT-based imaging biomarker which would allow for visualization and quantification of COPD phenotypes. Previously, we developed the parametric response map (PRM) as a voxel-based method for improving the sensitivity of diffusion-MRI data for identifying early therapeutic response in glioma patients.¹⁶ This technique has since been validated as an early surrogate imaging biomarker of survival for gliomas, head and neck cancer, breast cancer and metastatic prostate cancer to the bone.¹⁷⁻²⁰ In 2009, we also demonstrated using temporal perfusion-MRI that PRM is a generalized method, not restricted to diffusion, for assessing early clinical outcome in cancer patients.²¹ Here we have considerably modified the PRM analytical approach in order to leverage the power of its pairwise analysis on inspiratory and expiratory CT lung scans to allow for quantification of functional small airways disease separately from

emphysema which is not possible when analyzed independently. Our proposed PRM method is therefore a unique quantitative biomarker approach for assessment of COPD severity, phenotype and spatial heterogeneity using CT images. There are three fundamental steps in applying PRM to CT data prior to clinical diagnosis (Fig. 1). These steps involve image acquisition, co-registration and finally classification of voxels as consisting of lung parenchyma that is normal (green), functional small airways disease (fSAD; yellow) or emphysema (red). The PRM method proposed in this study is a fundamentally new and distinct application from prior work using this technique and a distinctly different approach from other CT-based quantitative measures (see Supplemental Introduction). Commonly used CT metrics for diagnosis of lung disease use tissue volumetric summary statistics of lung fields such as the percentage of emphysema and mean lung density (MLD) from inspiratory and expiratory phases. PRM however, classifies local variations in lung function based on a voxel-by-voxel comparison of lung attenuation changes from digitally co-registered inspiratory and expiratory CT scans to provide both global and local evaluation of COPD severity and phenotype. Using a well-defined COPD cohort, we show that this methodology allows for detection and quantification of not only emphysema but also tissue that comprise small airways disease that can be monitored longitudinally in a single unified approach. PRM, with the ability to distinguish the relative contributions of fSAD and emphysema in COPD phenotypes, may serve as a complementary readout to current pulmonary function tests (PFTs) and CT-based metrics that will allow for more accurate diagnosis and improve the treatment management of individual patients.

Results

Inspiratory and expiratory CT scans were acquired from 10,000 subjects as part of the COPDGene study. Of these, 194 with varying GOLD status (Supplemental Table 1) were used to demonstrate the PRM method for quantifying fSAD and emphysema. The strength of PRM to identify individuals with varying phenotypes of COPD is demonstrated in representative coronal PRM images with corresponding inspiratory and expiratory CT scans from four subjects with varying GOLD status (Fig. 2). Details on the classification scheme are provided in the Methods and Supplement (Supplemental Figure 1). Table 1 provides an exemplary comparison of PRM values to spirometry and non-PRM CT metric of emphysema for each of the four chosen subjects. In the extreme cases, FEV₁ and percentage of emphysema, defined as percentage of lung < -950 (% emphysema in Table 1), accurately assess the severity of COPD, with Subject A and D consisting of low and high levels, respectively, of emphysema as observed in Fig. 2. Where PRM is most useful is in the identification of the underlying COPD phenotypes and the location of the specific disease classifications. Subjects B and C were found to have near identical FEV₁ measurements yet the percentage of emphysema was elevated in the Subject C compared to Subject B. Current techniques for assessing COPD severity are unable to accurately diagnosis Subject B leaving clinicians to presume based on FEV₁ and percentage of emphysema that COPD for this individual is due primarily to airways obstruction. Our PRM measurements revealed that 26% of the lung tissue of Subject B consisted of fSAD (PRM^{fSAD}) tissue localized primarily in the upper lobes of both lungs with minimal signs of emphysema as denoted by PRM^{Emph}. In Subject C, emphysema has progressed throughout the upper left lung, identified by the

low attenuation on the inspiratory CT scan as a hallmark of emphysema. Current clinical diagnostic methods such as percentage of emphysema would have missed detection of fSAD expanding in the right upper lobe, which was easily identified, quantified and spatially displayed using PRM.

The unique ability of PRM to identify and track individual voxels from inspiratory and expiratory scans allows for the individual components of COPD to be quantified and monitored (see Supplemental Fig. 2). Note that the scatter plot of PRM^{fSAD} and PRM^{Emph} for all 194 subjects can be seen in Supplemental Fig. 3. PRM provided unique information on the contribution of fSAD and emphysema in a variety of clinical tests that have been identified as being prognostic of COPD (Supplemental Table 2). We also found our PRM metrics highly sensitive when modeling airway obstruction while controlling for other CT-based airway measurements (Supplemental Table 3).

An interesting trend was observed that involved the spatial distribution and association of fSAD tissue with emphysema (Fig. 3). PRM signatures for each individual were further analyzed to identify a pattern of disease progression in our cohort of 194 subjects. As part of the PRM approach, each voxel is classified based on their location within a coordinate system. Depicted in Fig. 3a (see Supplemental Results for details) is the distribution of voxels with varying values at inspiration and expiration for a subject with Normal status as determined by spirometry ($\text{FEV}_1/\text{FVC} = 83\%$, $\text{FEV}_1 = 81\%$). Most of the voxels reside within the Normal lung classification of PRM (green field) with voxels generally having more attenuation at expiration than inspiration as indicated by the hyperintensity of the expiration CT scan (Fig. 3a right panel). In contrast, an individual with GOLD 4 status ($\text{FEV}_1/\text{FVC} = 25\%$, $\text{FEV}_1 = 18\%$) was found to have a PRM signature distinct from the Normal status. For this individual voxels reside primarily within fSAD (yellow field) and emphysema (red field) classifications. Similar attenuation on CT scans at inspiration and expiration and extensive emphysema (33% based on COPDGene percentage of emphysema metric) was observed (Fig. 3b right panel), which is characteristic of an individual with dyspnea (MMRC Dyspnea Scale = 3). As observed for these two subjects, voxels tend to concentrate on the Cartesian plot (i.e. PRM signature), with red and blue regions denoting high and low voxel density/number, respectively, such that an elliptical pattern is generated that has a location, distribution and orientation that is unique for each individual. Based on the distribution of voxels (Fig. 3a and 3b), we calculated for each subject the center of distribution (CoD) that is the median values of all voxel data for both axes (position of the arrows) and the direction of largest covariance component, i.e. the principal eigenvector which designates the longest axes of the ellipse, of each subject's scatter plot (arrows; direction of arrowheads are arbitrarily chosen) and plotted data from all individuals on the inspiration-expiration diagram (i.e. Cartesian plot), which consists of the three PRM color-codes defined in Fig. 1. What we observed is a pattern suggestive of COPD progression that has never been demonstrated previously by CT-based measures. In fact, the data from the 194 subjects studied suggests that fSAD precedes emphysema in the progression of COPD. Another presentation of this trend is demonstrated in Supplemental Fig. 3. Here PRM^{fSAD} was plotted against PRM^{Emph} for all 194 subjects. The color legend identifies the GOLD status of each individual. As seen in the Supplemental Fig. 3, many subjects have less than 10% emphysema yet some can have fSAD that make up 10–30% of their lung parenchyma.

What is also interesting about this plot is there appears to be a plateau in the amount of fSAD that can be present in the lung. More severe lung obstruction as determined by FEV₁ (GOLD 3 and 4) appears to be attributed to contributions of both fSAD along with emphysema, with PRM^{fSAD} plateauing around 40–50% and PRM^{Emph} increasing to > 20% of the lung volume. This figure emphasizes the relationship between fSAD and emphysema that provides information similar to Fig. 3. Our findings agree with the recent work by Hogg's group, which have demonstrated by pathology of the narrowing and disappearance of small airways prior to the onset of emphysema in COPD subjects.²² It is important to note what we are presenting in Fig. 3c and Supplemental Fig. 3 are not longitudinal data but rather snap shots of a cohort of individual subjects at various stages of the disease. What is significant about this finding obtained from this heterogeneous population is that a specific trend in the CT data was observed by our PRM methodology that suggests that airway obstruction associated with fSAD appears to be a precursor to the development of emphysema.

In order to provide some insight into the feasibility of PRM as an imaging biomarker to monitor individuals longitudinally over time we obtained additional retrospective imaging data outside of the COPDGene study from subjects who had previously visited our University of Michigan pulmonary clinic and underwent inspiratory/expiratory CT scanning protocol over a period of time. Shown in Fig. 4 are examples of two different subjects along with the time intervals between CT exams, PRM metrics normal (green), fSAD (yellow) and emphysema (red) provided as relative volumes along with FEV₁ (Fig. 4 legend) acquired as a standard PFT. The subject which had considerable emphysema and fSAD at the baseline scan (month 0), had at 11 months later progressive emphysema greater than the loss of fSAD as there was an additional loss of normal functional lung as well (Fig. 4a). FEV₁ was unchanged from 18% to 17% over this time interval. These two pathologies appear to co-exist in high percentages throughout the disease duration of this subject. In contrast, Fig. 4b reveals a COPD subject with a largely asthmatic component with no emphysema. Over a 26 month period, the amount of normal lung increased corresponding with a decrease in fSAD along with an increase in FEV₁ from 66 to 75%. These human examples reveal the significant potential of using PRM to monitor COPD over time to provide a phenotype classification basis for patient response or progression.

Discussion

In this study we demonstrate the ability of PRM as a novel application of an existing voxel-based image post-processing technique, to serve as a quantitative imaging biomarker to assess phenotypic contributions of fSAD and emphysema in COPD when applied to inspiratory and expiratory CT images.²¹ The novelty of this application of PRM over what has been done previously is that cyclic physiological respiratory states, not changes in biological tissue as a response to disease or treatment, are being captured through imaging and compared on a voxel-by-voxel basis by image co-registration. The registered CT images now share the same geometric space, i.e. lung tissue at expiration is spatially aligned with the same lung tissue at inspiration. A unique classification scheme based on specific thresholds was developed that allows for spatial information about the disease to be retained. This is accomplished by classifying voxels into discrete zones that can be analyzed as a

global metric (i.e. relative volumes) but also supports the ability to identify local phenomena of the individual PRM metrics. Not only can PRM be used as a versatile imaging biomarker to diagnose disease extent and phenotype, but it also can provide detailed spatial information related to disease distribution and precise location. Moreover, PRM could potentially be used to reveal the nature of COPD progression as it pertains to small airways disease and emphysema.

The natural history of COPD has been primarily based on pulmonary function tests.²³ Although the breadth of this knowledge has provided detailed information used to improve patient clinical care, it does not address the progression of the underlying phenotypes of COPD.²⁴ Such understanding would allow clinicians to tailor therapeutic intervention to a particular COPD phenotype as most cases have fSAD and emphysema thus prescribing the optimal treatment for an individual. An important feature of PRM not easily attained by other methodologies is the potential to localize the disease states and possibly detect and identify the COPD progression pathway. This is made possible through the unique PRM signature for each individual and the sufficiently large population available for this analysis. When plotting the metrics center of distribution (CoD) and principle eigenvector for each of the 194 subjects, we observed not a random distribution of values within our inspiration-expiration plot (i.e. Cartesian plot) but a continuous ribbon originating from healthy lung, though fSAD and ending at emphysema (Fig. 3). Since each arrow is only a snap-shot of disease state, we acquired additional longitudinal data from individuals not accrued as part of the COPDGene study to demonstrate the utility of PRM as an imaging biomarker for monitoring changes in COPD phenotype (Fig. 4). Although promising, further validation of the use of PRM at following COPD progression in subjects will need to be performed using a larger cohort of imaging data collected from a longitudinal study. Nevertheless these results are very promising in that PRM provides a tool for improving our understanding of the relationship between fSAD and emphysema in COPD progression in individuals.

Another potential use of this technique is as a secondary biomarker of therapeutic response in pharmacological trials. Few pharmaceutical advances have been made over the past few decades, primarily due to the lack of accurate biomarkers of COPD.^{25,26} In an effort to rigorously test potential therapies for COPD, the US Food and Drug Administration has set guidelines for potential biomarkers in specific contexts which include stratification of patient populations, dose-ranging and use as a disease outcome. Currently, no well-validated biomarker of COPD has been identified other than FEV₁, which is still limited. Inclusion of the PRM approach proposed herein as a secondary endpoint may aid in pharmacological trials by stratifying patients with fSAD or emphysema dominant COPD (Fig. 3, 4 and Supplemental Fig. 3) as well as therapeutic response or disease progression (Fig. 4). For example, it could be envisioned that the relative volume of fSAD lung tissue (yellow voxels) could be used as a surrogate of treatment efficacy in routine patient care and in drug trials. A change of yellow voxels into green voxels should indicate lung tissue which has been rescued by therapeutic intervention.

What distinguishes the PRM approach from what has been previously accomplished is the classification process imposed on individual voxels which allows us to capture a unique signature specific to the disease state of an individual patient. To date, groups who evaluate

the prognostic value of registered data sets typically use statistically based metrics, such as the mean of the Jacobian, differences in HU or dissimilarity measures based on the histograms of the CT images where information from the measure is pooled throughout the lung into a single outcome measure which forfeits the spatial information that is inherent in the CT images^{9,10,14,27}.

Given the prevalence and impact of COPD worldwide there is a crucial need to develop quantitative imaging methodologies, which can more objectively characterize the disease and, ideally, define response to therapy. PRM provides a quantitative imaging application that has promise in classifying COPD by disease subtype which can be applied to facilitate individualized treatment strategies. PRM provides for parenchymal analysis as well as analysis of lung airway disease through a systematic algorithmic workflow for quantification of lung function in a high volume, time constrained clinical environment.

Methods

Subjects from COPDGene study

Subjects (n=194, 110/84 M/F) with at least a 10 pack-year history of cigarette smoking were enrolled as part of the 10,000 total accrued subjects previously described COPDGene Study (www.copdgene.org)³. The COPDGene Study research protocol was approved by the University of Michigan Institutional Review Board, and all participants provided written informed consent. Subject characteristics and COPDGene Study details are summarized in Supplemental Table 1.

Additional subjects

Additional retrospective longitudinal imaging data outside of the COPDGene study from two subjects who had previously visited our University of Michigan pulmonary clinic and underwent inspiratory/expiratory CT scanning protocol over two time intervals. Acquisition and analysis of this data was approved by our Institutional Review Board.

CT acquisition and analysis

Except for the additional subjects obtained for longitudinal analysis, all CT data and analysis were performed as part of the COPDGene project. Whole-lung volumetric multi-detector CT acquisition was performed at full inspiration and normal expiration using a standardized previously published protocol.³ Data reconstructed with the standard reconstruction kernel was used for quantitative analysis. All CT data were presented in Hounsfield Units (HU), where stability of CT measurement for each scanner was monitored monthly using a custom COPDGene phantom.³ For reference, air and water attenuation values are -1000 and 0 HU; healthy lung parenchyma is approximately -700 HU. Quantitative analysis of emphysema severity was performed on segmented lung images using Slicer (www.Slicer.org). The percentage of emphysema (% emphysema) was defined as all lung voxels with a CT attenuation value of less than -950 Hounsfield units (HU) divided by the total lung volume at full inflation, multiplied by 100. The total percent gas trapping (GT) was defined as the fraction of lung with a CT attenuation value of less than -856 HU divided by the total lung volume at expiration, multiplied by 100. Automated airway analysis was performed using

VIDA Pulmonary Workstation version 2.0 (www.vidadiagnostics.com) using previously validated segmentation methods (details in Supplemental Methods).²⁸ All analytical measurements not pertaining to the discussed PRM approach were performed by COPDGene personnel. Similar data acquisition and post-processing were performed on the additional retrospective longitudinal data sets which were not obtained as part of the COPDGene study.

Parametric response mapping (PRM)

Prior to registration, lung parenchyma and airways were segmented to restrict the focus of the registration process to the lungs only. The expiration CT (floating) image is spatially aligned to the inspiration (reference) CT image using thin plate splines as the deformable registration interpolant. The registration algorithm is manually initialized using 42 degrees of freedom (DOF) warping of the floating dataset. The automatic algorithm then iteratively optimizes the solution using mutual information as the objective function. The DOF of the warping is roughly doubled and the scale space halved in each of three subsequent registration cycles automatically increasing the warping of the floating dataset ultimately to approximately 330 DOF with no folding²⁹.

The Parametric Response Map of quantitative CT as expressed in HU, a measure of tissue density, was determined by imposing two thresholds: 1) -950 HU on full inspiration scan with values less denoted emphysema and 2) -856 HU on normal expiration scan with values less denoted gas trapping. These thresholds are applied to a joint histogram formed using all voxel pairs within the registered inspiration-expiration lungs. Three discrete classifications were identified (details in the Supplemental Methods) where voxels were designated as: healthy lung parenchyma color coded green, functional small airways disease (fSAD) color coded yellow and emphysema color coded red. Global measure were also determined and presented as the relative volumes of each class, which are the sum of all voxels within a zone normalized to the total lung volume. To minimize the contribution of airways and vessels in our PRM analysis of parenchyma, only voxels with HU between -500 HU to -1000 HU in both scans were considered for analysis.

Data and statistical analyses

Bivariate linear and logistic regression models were generated for individual prognostic indices of COPD severity and overall survival to assess the contribution of fSAD and emphysema, as quantified by PRM^{fSAD} and PRM^{Emph} , respectively. *P* values for the various statistical tests performed are presented in Supplemental Table 2. In addition, multivariate linear regression models were generated for FEV_1 and FEV_1/FVC to assess the contributions of PRM^{fSAD} , PRM^{Emph} , and airway measurements WAP, IAI, Pi10 and AWT to the models. All statistical computations were performed with a statistical software package (SPSS Software Products). Results were considered statistically significant at the two-sided 5% comparison-wise significance level ($P < 0.05$). All data is presented as the mean \pm the standard error of the mean. Details on PRM signature analyses are presented in Supplemental Statistics. All calculations were performed using a mathematical programming software package (MatLab, The MathWorks, Inc.).

Supplementary Material

Refer to Web version on PubMed Central for supplementary material.

Acknowledgments

We would like to acknowledge S. Sarkar, M. Bule and S.A. Blanks for their indispensable contribution in processing the CT data sets. We would also like to acknowledge D.A. Lynch, MD and the COPDGene investigators for providing the CT scans from National Jewish Health and recruiting the subjects included in this analysis. This work was supported by the US National Institutes of Health research grant P50CA93990 and COPDGene grants U01HL089897 and U01HL089856. J.L.B. is a recipient of support from the NIH training grant T32EB005172

References

1. Buist AS, et al. The Burden of Obstructive Lung Disease Initiative (BOLD): rationale and design. *COPD*. 2005; 2:277–283. [PubMed: 17136954]
2. Agusti A, Vestbo J. Current Controversies and Future Perspectives in COPD. *Am J Respir Crit Care Med*. 2011
3. Regan EA, et al. Genetic epidemiology of COPD (COPDGene) study design. *COPD*. 2010; 7:32–43. [PubMed: 20214461]
4. Han MK, et al. Chronic obstructive pulmonary disease phenotypes: the future of COPD. *Am J Respir Crit Care Med*. 2010; 182:598–604. [PubMed: 20522794]
5. Gevenois PA, de Maertelaer V, De Vuyst P, Zanen J, Yernault JC. Comparison of computed density and macroscopic morphometry in pulmonary emphysema. *Am J Respir Crit Care Med*. 1995; 152:653–657. [PubMed: 7633722]
6. Gevenois PA, et al. Comparison of computed density and microscopic morphometry in pulmonary emphysema. *Am J Respir Crit Care Med*. 1996; 154:187–192. [PubMed: 8680679]
7. Newman KB, Lynch DA, Newman LS, Ellegood D, Newell JD Jr. Quantitative computed tomography detects air trapping due to asthma. *Chest*. 1994; 106:105–109. [PubMed: 8020254]
8. Eda S, et al. The relations between expiratory chest CT using helical CT and pulmonary function tests in emphysema. *Am J Respir Crit Care Med*. 1997; 155:1290–1294. [PubMed: 9105069]
9. Gorbunova V, et al. Early detection of emphysema progression. *Med Image Comput Comput Assist Interv*. 2010; 13:193–200. [PubMed: 20879315]
10. Gorbunova V, et al. Weight preserving image registration for monitoring disease progression in lung CT. *Med Image Comput Comput Assist Interv*. 2008; 11:863–870. [PubMed: 18982686]
11. Kubo K, et al. Expiratory and inspiratory chest computed tomography and pulmonary function tests in cigarette smokers. *Eur Respir J*. 1999; 13:252–256. [PubMed: 10065664]
12. Matsuoka S, et al. Quantitative assessment of air trapping in chronic obstructive pulmonary disease using inspiratory and expiratory volumetric MDCT. *AJR Am J Roentgenol*. 2008; 190:762–769. [PubMed: 18287450]
13. Matsuoka S, Kurihara Y, Yagihashi K, Nakajima Y. Quantitative assessment of peripheral airway obstruction on paired expiratory/inspiratory thin-section computed tomography in chronic obstructive pulmonary disease with emphysema. *J Comput Assist Tomogr*. 2007; 31:384–389. [PubMed: 17538284]
14. Reinhardt JM, et al. Registration-based estimates of local lung tissue expansion compared to xenon CT measures of specific ventilation. *Med Image Anal*. 2008; 12:752–763. [PubMed: 18501665]
15. Li B, Christensen GE, Hoffman EA, McLennan G, Reinhardt JM. Pulmonary CT image registration and warping for tracking tissue deformation during the respiratory cycle through 3D consistent image registration. *Med Phys*. 2008; 35:5575–5583. [PubMed: 19175115]
16. Moffat BA, et al. Functional diffusion map: a noninvasive MRI biomarker for early stratification of clinical brain tumor response. *Proc Natl Acad Sci U S A*. 2005; 102:5524–5529. [PubMed: 15805192]

17. Galban CJ, et al. A feasibility study of parametric response map analysis of diffusion-weighted magnetic resonance imaging scans of head and neck cancer patients for providing early detection of therapeutic efficacy. *Transl Oncol.* 2009; 2:184–190. [PubMed: 19701503]
18. Hamstra DA, et al. Functional diffusion map as an early imaging biomarker for high-grade glioma: correlation with conventional radiologic response and overall survival. *J Clin Oncol.* 2008; 26:3387–3394. [PubMed: 18541899]
19. Ma B, et al. Voxel-by-voxel functional diffusion mapping for early evaluation of breast cancer treatment. *Inf Process Med Imaging.* 2009; 21:276–287. [PubMed: 19694270]
20. Reischauer C, et al. Bone metastases from prostate cancer: assessing treatment response by using diffusion-weighted imaging and functional diffusion maps—initial observations. *Radiology.* 2010; 257:523–531. [PubMed: 20829534]
21. Galban CJ, et al. The parametric response map is an imaging biomarker for early cancer treatment outcome. *Nat Med.* 2009; 15:572–576. [PubMed: 19377487]
22. McDonough JE, et al. Small-airway obstruction and emphysema in chronic obstructive pulmonary disease. *N Engl J Med.* 2011; 365:1567–1575. [PubMed: 22029978]
23. Kohansal R, Soriano JB, Agusti A. Investigating the natural history of lung function: facts, pitfalls, and opportunities. *Chest.* 2009; 135:1330–1341. [PubMed: 19420200]
24. Oga T, et al. Multidimensional analyses of long-term clinical courses of asthma and chronic obstructive pulmonary disease. *Allergol Int.* 2010; 59:257–265. [PubMed: 20657164]
25. Cazzola M, et al. Outcomes for COPD pharmacological trials: from lung function to biomarkers. *Eur Respir J.* 2008; 31:416–469. [PubMed: 18238951]
26. Martinez FJ, Donohue JF, Rennard SI. The future of chronic obstructive pulmonary disease treatment—difficulties of and barriers to drug development. *Lancet.* 2011; 378:1027–1037. [PubMed: 21907866]
27. Yamamoto T, et al. Investigation of four-dimensional computed tomography-based pulmonary ventilation imaging in patients with emphysematous lung regions. *Phys Med Biol.* 2011; 56:2279–2298. [PubMed: 21411868]
28. Hu S, Hoffman EA, Reinhardt JM. Automatic lung segmentation for accurate quantitation of volumetric X-ray CT images. *IEEE transactions on medical imaging.* 2001; 20:490–498. [PubMed: 11437109]
29. Meyer CR, et al. Demonstration of accuracy and clinical versatility of mutual information for automatic multimodality image fusion using affine and thin-plate spline warped geometric deformations. *Med Image Anal.* 1997; 1:195–206. [PubMed: 9873906]

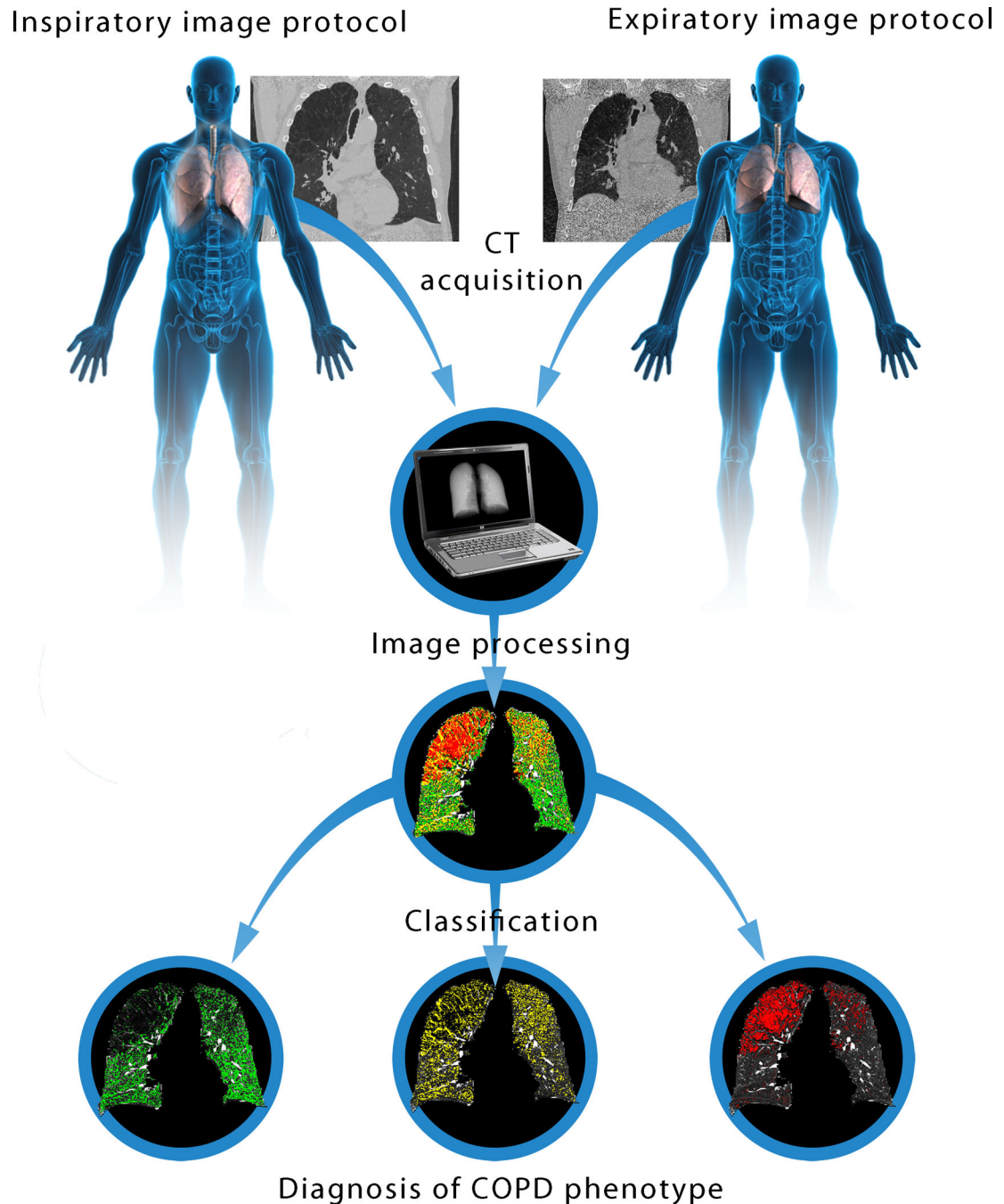


Figure 1. Schematic diagram of the PRM method

PRM is a fundamentally distinct approach from conventional CT-based quantitative measures. This methodology classifies lung attenuation maps on a voxel-by-voxel basis through image co-registration of inspiratory and expiratory images to provide a global measure as well as local distribution and extent of COPD phenotypes. The PRM method consists of four key steps: image acquisition, image processing, quantification and classification. Acquisition of CT scans was performed using imaging protocols that emphasize high resolution with sufficient signal-to-noise on both serial CT scans as defined

by the COPDGene Study. Image Processing primarily consists of lung segmentation followed by deformable volumetric registration. Deformable Registration spatially aligns the expiration scan to the inspiration scan such that both share the same spatial geometry. Segmentation of the lung bronchus from the parenchyma is required for further analysis. Classification of voxels from attenuation maps into discrete zones allows for the quantification of global measures of normal parenchyma ($\text{PRM}^{\text{Normal}}$, green), functional small airways disease (PRM^{fSAD} , yellow) and emphysema (PRM^{Emph} , red) that is highly sensitive to the extent of COPD as well as retaining spatial information for analysis of the distribution of disease within the lung. The PRM method is a sensitive prognostic imaging biomarker capable of elucidating the complexity and severity of COPD.

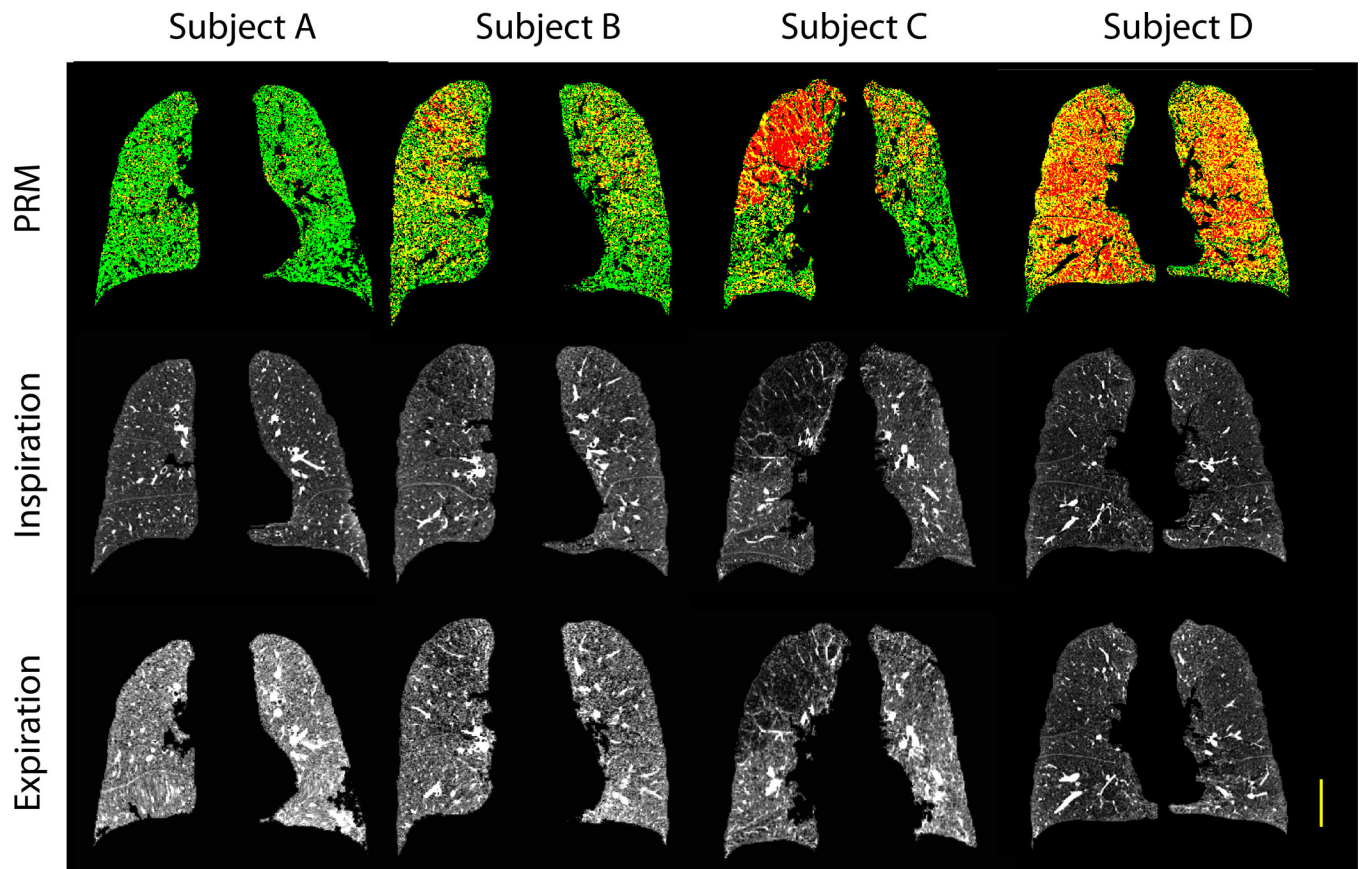


Figure 2. COPD phenotypes identified by PRM

The strength of PRM to identify functional small airways disease (PRM^{fSAD}) from emphysema (PRM^{Emph}) is demonstrated in representative sagittal PRM images with corresponding inspiratory and expiratory CT scans from four individuals with varying GOLD status. From the three classifications, normal lung tissue is denoted green, fSAD is denoted yellow, and emphysema is denoted red. Yellow line indicates 5 cm. Additionally, a modified figure has also been provided for easier visualization for those with some forms of color blindness (Supplemental Figure 4).

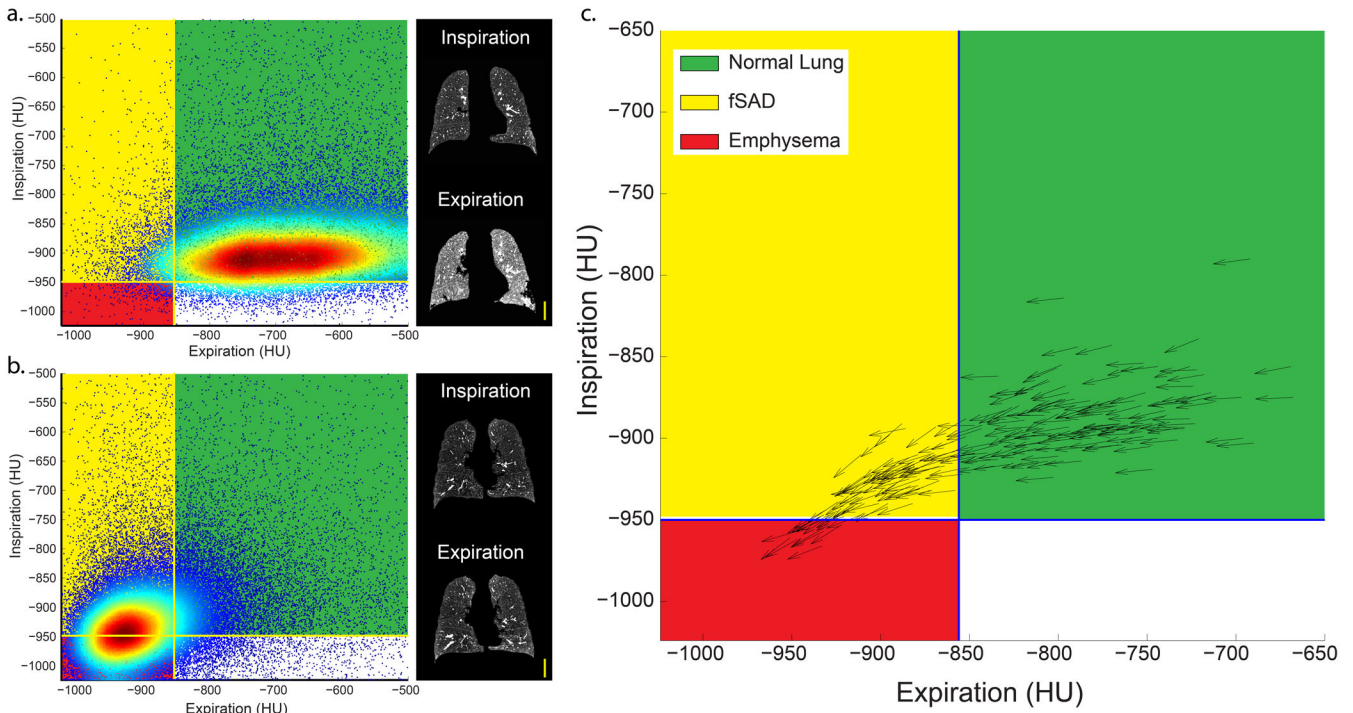


Figure 3. COPD progression as determined by PRM

A plot of the registered inspiration and expiration CT values for all voxels in the parenchyma provides a signature (i.e. distribution and location of voxel values on a X-Y plot) unique to the COPD severity in the studied subjects. To identify the extent and phenotype of the disease, voxels are classified as normal lung (Green), function small airways disease (fSAD), or emphysema based on two thresholds: 1) -950 HU on inspiration scan (horizontal solid line) with values less denoted emphysema and 2) -856 HU on expiration scan (vertical solid line) with values less denoted gas trapping. **(a)** Depicted is the distribution of voxels with varying values at inspiration and expiration for an individual with Normal status as determined by spirometry ($FEV_1/FVC = 83\%$, $FEV_1 = 99\%$). Most of the variation in lung attenuation is observed along the expiration, with voxels generally having less attenuation at expiration than inspiration (right panel presents sagittal slices of CT images at inspiration and expiration). The distribution of voxels generates an elongated elliptical pattern with voxels highly concentrated in the center (red) and decreasing on the periphery (blue). Most voxels are classified as normal lung. **(b)** A subject with GOLD 4 status ($FEV_1/FVC = 25$, $FEV_1 = 18$) is found to have a signature apart from the Normal status where voxels are classified primarily as fSAD or emphysema. For this subject the PRM signature is less elongated than the pattern observed for the subject without COPD. Similar attenuation on CT scans at inspiration and expiration is observed (right panel), which is characteristic of a subject with extensive emphysema. **(c)** As observed for the two cases **(a)** and **(b)**, a unique attribute of PRM is the distinct signature, distribution and location, of the voxels in the Inspiration-Expiration plots. Calculation of the center of distribution (CoD) that is the median value for both axes (position of the arrows) and principal eigenvector of the data determined by the principal component analysis (arrows) provide information on location and direction of the principal distribution, respectively. A plot of

these two metrics for each subject with the three PRM color-codes for COPD are demonstrated. A distinct pattern of COPD progression was revealed suggesting that functional small airways disease (yellow) precedes emphysema (red) in the progression of COPD. Yellow line indicates 5 cm.

Author Manuscript

Author Manuscript

Author Manuscript

Author Manuscript

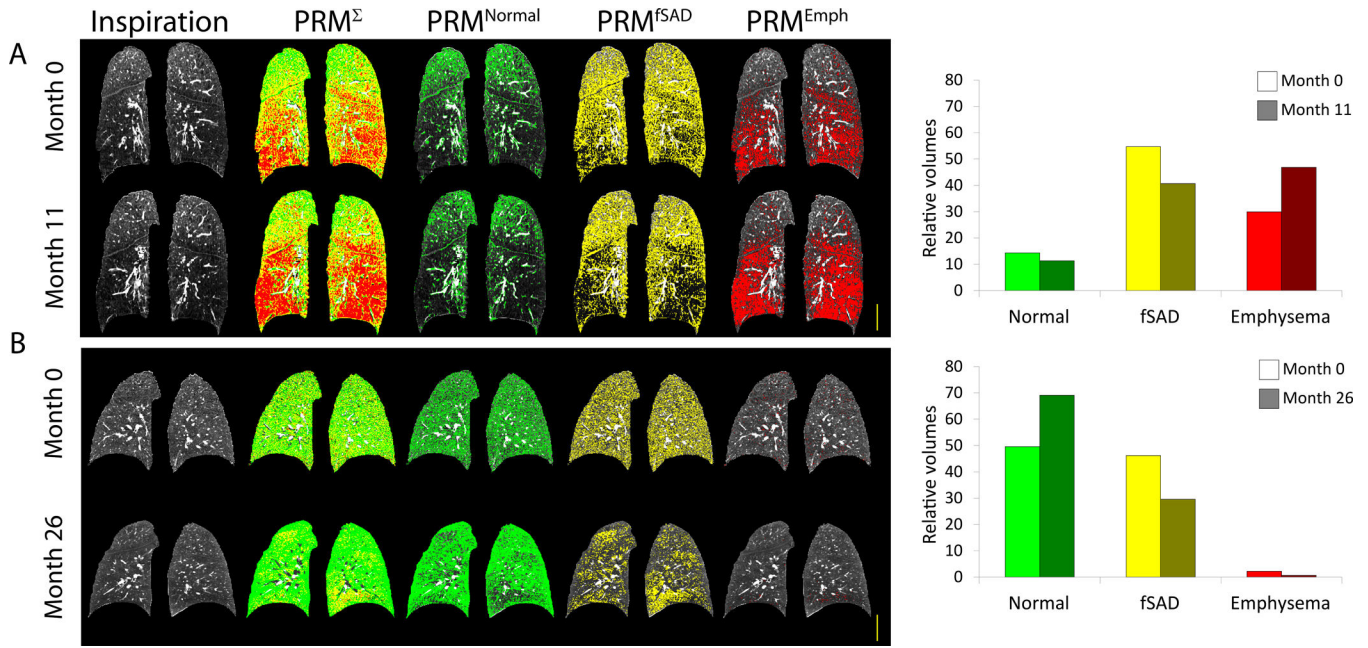


Figure 4. PRM as an imaging biomarker of COPD progression
 PRM is a highly sensitive technique for identifying the contribution of fSAD and emphysema within an individual. Demonstrated on two subjects, not part of the COPDGene study, is the utility of PRM as an imaging biomarker of disease progression. **(a)** Serial CT data acquired 325 days apart from an individual identified as GOLD 4 was analyzed by PRM. Within the first CT examination, PRM identified extensive fSAD (PRM^{fSAD}; yellow) and emphysema (PRM^{Emph}; red) throughout the lungs. Analysis of the follow-up CT examination by PRM showed a drop in fSAD and an increase in emphysema suggesting a transition of the disease to a more severe state. Conventional spirometry was unable to observe any changes in the subject’s condition with FEV₁(%) of 18% and 17% 11 months later. **(b)** The main contributing factor of the flow obstruction in an individual with GOLD 2 status was found by PRM to be fSAD and not emphysema. Analysis of follow-up scans by PRM showed a reduction in fSAD (PRM^{fSAD}; yellow) and an improvement in normal lung (PRM^{Normal}; green). This is consistent with the reduction in flow obstruction determined by spirometry with FEV₁(%) of 66% to 75% at follow-up. Yellow line indicates 5 cm.

Table 1

Subject measures

Subject	A	B	C	D
GOLD	NA	2	2	4
FEV ₁	99	55	59	18
% Emphysema	4	5	19	23
PRM ^{Normal}	85	66	54	21
PRM ^{Emph}	1	4	16	28
PRM ^{fSAD}	6	26	22	45

Note: NA refers to not applicable. % Emphysema is the relative volume of lung with attenuation < -950 HU on the inspiratory scan.